An Analysis on Induced Numerical Oscillations by Lax–Friedrichs Scheme

Article *in* Differential Equations and Dynamical Systems · July 2016

DOI: 10.1007/s12591-016-0311-0

CITATION
1

READS
198

2 authors:

Ritesh Dubey
SRM Institute of Science and Technology
21 PUBLICATIONS **74** CITATIONS
SEE PROFILE

Biswarup Biswas
Indian Institute of Technology Delhi
7 PUBLICATIONS **17** CITATIONS
SEE PROFILE

An analysis on induced numerical oscillations by Lax-Friedrichs scheme *

Ritesh Kumar Dubey† and Biswarup Biswas
Research Institute, SRM University, Tamilnadu
India

Abstract

Induced numerical oscillations in the computed solution by monotone schemes for hyperbolic conservation laws has been a focus of recent studies. In this work using a local maximum principle, the monotone stable Lax-Friedrichs(LxF) scheme is investigated to explore the cause of induced local oscillations in the computed solution. It expounds upon that LxF scheme is locally unstable and therefore exhibits induced such oscillations. The the carried out analysis gives a deeper insight to characterize the type of data extrema and the solution region which cause local oscillations. Numerical results for benchmark problems are also given to support the theoretical claims.

keywords: hyperbolic conservation laws, Local oscillations, numerical stability, finite difference schemes.
AMS classification35L65,65M10,65M06,65M12.

1 Introduction

The numerical computation of hyperbolic conservation laws has been a focus of study for researcher working on modelling and simulation of many physical problems in Physics, Gas-dynamics, hydro dynamics etc. In one dimensional case a typical scalar conservation law can be written as

$$u_t(x,t) + f_x(u(x,t)) = 0,\ (x,t) \in R \times R^+ \quad (1)$$

$$u_0(x) = u(x,0). \quad (2)$$

The conserved variable $u = u(x,t) \in R$ is a function of spatial and temporal variables x and t respectively, $f(u) \in R$ is smooth flux function associated with (1). The characteristic speed associated with (1) is given by $f^{'}(u) = \dfrac{\partial}{\partial u} f(u)$. There are classical results and well established theory for the stable and convergent numerical approximation for the scalar conservation law (2), [10, 4, 18, 17, 13]. It is well known that the exact solution $u(x,t)$ of (1) satisfies the global maximum principle [21] i.e., if $m = \min\limits_x u_0(x), M = \max\limits_x u_0(x)$ then

$$u(x,t) \in [m, M],\ \forall x \text{ and } t > 0. \quad (3)$$

It is therefore desirable for any numerical scheme to yield a stable solution of (1) in the sense of maximum principle i.e., the maxima or minima in the initial solution should not increase or decrease

*Carried out work is financially supported by DST India through project # SR/FTP/MS-015/2011
†mail-to: riteshkd@gmail.com; riteshkumar.d@res.srmuniv.ac.in

respectively at later time. The non-linearly stable monotone and total variation diminishing (TVD) schemes for (1) strictly follow the maximum principle. A monotone method ensures that a monotone data sequence will map to a new monotone data sequence however such preservation property does not hold for non-monotone solution profile e.g. monotone data profile to the left and right of the local extremum [3]. On the other hand the total variation of a discrete solution u is defined as

$$TV(u) = \sum_{i=-\infty}^{i=\infty} |u(x_{i+1}, t) - u(x_i, t)| \tag{4}$$

where x_{i+1} and x_i are the consecutive grid points of the computational mesh as defined below. It is clear from (4) that total variation of the function u can only be effected by maxima or minima and any formation of new local maximum-minimum pair always increase the total variation [8]. Considering (4) the total variation diminishing stability is defined i.e., $TV(u(x,t)) \leq TV(u(x,0))$ which ensures that maxima or minima in the initial data sequence can not increase or decrease at later time. Moreover TVD implies monotonicity preservation. Therefore it is obviously expected that the numerical approximation by a monotone or TVD scheme will be oscillations free. Contrary to the expectations, phenomena of *introduction of local oscillations* at extrema are observed in the numerical solution by monotone or TVD schemes [9, 12, 2, 3, 14, 15].

In this work, the focus is on the numerical oscillations by Lax-Friedrichs (LxF) scheme. The strongest point of this work is the rudimentary argument which is used to give further understanding of the effect of local extrema, data ratio and CFL number on the induced local oscillations by Lax-Friedrichs (LxF) scheme. In section 2, a brief detail is given on the state of the art addressing the problem of induced oscillations by LxF scheme [9, 12, 2, 3, 14, 15]. Further details are also given to show the gaps which are needed to be filled in the explanation for such oscillatory phenomena in section 2.1. In section 3, using upwind range condition a stronger stability condition is defined which ensures non-occurrence of new extrema. The LxF scheme is analyzed for such stronger stability. It is done by introducing a parameter which measures the smoothness of solution data and known as smoothness parameter. Carried out analysis discloses that LxF scheme is locally oscillatory. More precisely discussion in section 3.1 elucidate upon,

1. The dependence of the induced oscillations by LxF scheme on CFL number $a\lambda$ (or τ).
2. Characterize the type of data extrema and the solution region which cause induced oscillations.
3. Numerical way to avoid step-wise approximation by LxF scheme for discontinuous solution region.

In section 4, numerical results are given for the scalar problems to support discussion and deduced local instability region of LxF scheme in section 2 and section 3 respectively.

Let h and τ denote the spatial and temporal step size respectively of the computational mesh defined by the grid points (x_i, t_n) where $x_i = ih$, $x_{i+\frac{1}{2}} = \frac{1}{2}(x_i + x_{i+1})$ and $t_n = n\tau,\ i \in \mathbb{Z},\ n \in \mathbb{N}$. In this setting the LxF scheme for scalar problem (1) is given by,

$$u_i^{n+1} = \frac{1}{2}(u_{i+1}^n + u_{i-1}^n) - \frac{\tau}{2h}(f(u_{i+1}^n) - f(u_{i-1}^n)), \tag{5}$$

where $\lambda = \frac{\tau}{h}$, u_i^n denotes either point value $u(x_i, t_n)$ or cell average $\frac{1}{h}\int_{x_{i-\frac{1}{2}}}^{x_{i+\frac{1}{2}}} u(x, t_n)$ of u. It is well known that under linear stability condition $\lambda \max_u |f^{'}(u)| \leq 1$, the Lax-Friedrichs scheme (5) is both monotone and total variation diminishing (TVD) [9].

2 Induced local oscillations by LxF

Recently, active research work is reported to explain the cause of induced local oscillations by LxF scheme (5). It is reported that LxF exhibits oscillations with the shortest possible wave length equal to twice of the space interval and these spurious oscillations are significantly visible for small CFL number $a\lambda$ and large space step h [9].

In [2], structure of the operator corresponding to monotone three points Lax-Friedrichs scheme is discussed. An algorithm for discretization of initial condition is also proposed therein to ensure number of extrema within the discretize initial data is non-increasing. Later in [3] oscillation conditions are derived using a data sequence with single data extrema[1]. These oscillation conditions are used to to explore the source of induced oscillations in Lax-Friedrichs scheme, Rusanov scheme and TVD Nessyahu-Tadmor scheme of [16]. It is shown that for the classical LxF scheme (5), the oscillation conditions derived therein are always fulfilled, independently of the actual time step τ, specific flux function $f(u)$ and data ratio.

In 2009, phenomena of local oscillations in solution of monotone or TVD schemes is further studied by an excellent investigation of the discrete Fourier decomposition of the initial data that trigger the checkerboard mode, highest frequency mode [14]. It is mentioned that even though oscillations are induced at local extrema, the global TVD property could be preserved due to the compensation by strong decrease in solution amplitude. The conclusion therein is, *local oscillations are caused by high frequency mode in the absence of sufficient dissipation to suppress them.*

More recently in 2011, an interesting heuristic modified equation model for conservative numerical schemes is proposed in [15]. For the analysis the solution u_i^n is decomposed in to smooth $u_i^{n,s}$ and oscillatory part $u_i^{n,o}$. A heuristic modified equation is derived for the perturbation $\tilde{u}_i^n$, introduced in to the oscillatory part $u_i^{n,o}$. The effect of dissipation is characterized as damping, neutrality and amplification of oscillatory modes. The proposed model is used to analyze oscillatory nature shown by some numerical schemes for non-linear problem using the criteria on the stability of the oscillatory solution. It is concluded in [15] that, *schemes with large coefficient of viscosity are prone to oscillations at data extrema*, see also [2, 3].

2.1 Further explanation is required

Consider the linear transport equation

$$\frac{\partial u(x,t)}{\partial t} + a\frac{\partial u(x,t)}{\partial x} = 0, \;\; a = 1, (x,t) \in [x_l, x_r] \times \; R^+ \tag{6}$$

along with

(a) Initial data sequence with single extrema: Consider the data sequence (7) similar to the one in [3] (Equation (12), Page 970) and a slight modified one (8).

$$\ldots u_0(-2h) = u_0(-h) = 0.2, \; u_0(0) = 1.0, \; u_0(h) = 0.6 = u_0(2h), \ldots \tag{7}$$

$$\ldots u_0(-3h) = u_0(-2h) = -0.1, u_0(-h) = 0.2, \; u_0(0) = 1.0, \; u_0(h) = 0.6 = u_0(2h), \ldots \tag{8}$$

(b) Smooth initial condition

$$u_0(x) = \sin^4(\pi x), \; x \in [-1, 1] \tag{9}$$

and periodic boundary condition.

[1] See oscillatory conditions (7), (8) and remark 1.2, on page 969 in [3].

(c) Impulsive condition i.e.,

$$u_0(x) = \begin{cases} 1 & x \in [1-h, 1] \\ 0 & else \end{cases}, x \in [0, 2] \tag{10}$$

and periodic boundary condition.

(d) Step like condition

$$u_0(x) = \begin{cases} 1 & x \leq -0.5, \\ 0 & else, \end{cases}, x \in [-1, 1] \tag{11}$$

and constant boundary condition.

Case (i) *Oscillation free approximation for smooth extrema:* Consider smooth initial condition (9) consisting extrema at $u_0(\pm 0.5) = 1$ which corresponds to high frequency mode. Note that LxF scheme has largest coefficient of viscosity [9], but it does not show any induced oscillations at smooth data extrema such as (9) see Figure 1. Though one may justify the non-occurrence

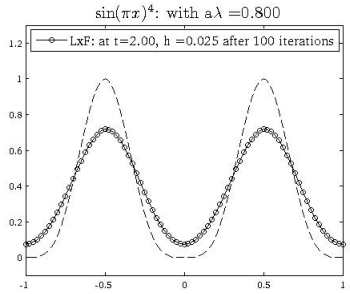

Figure 1: *No induced oscillation at smooth data extrema corresponding to highest frequency mode* $u(\pm 0.5, 0) = 1$ *by most dissipative LxF*

of oscillations by LxF scheme using conclusion from [14], that the local oscillations caused by high frequency mode are suppressed by sufficient dissipation of LxF scheme (5). Note that such explanation contradicts the occurrence of oscillations by LxF for high frequency mode corresponding to $u_i = 1$ for data (7) and impulsive initial data (10). Thus further exploration is required to justify the relation among high frequency modes, type of the extrema in solution and coefficient of dissipation of monotone schemes.

Case (ii) *The sensitivity of LxF on data ratio and CFL:* As remarked in [3], one may conclude that classical LxF scheme will always produce oscillations for data sequence with extrema similar to (7). Moreover these oscillations will be independent from the actual time step τ, specific flux function $f(u)$ and data ratio. In order to demonstrate that it is not always true, we consider the data sequences (7) and (8). It is clear from the numerical results shown in Figure 2 that approximation by LxF scheme produces oscillations for data sequence (7) but does not show oscillations for data sequence (8) in Figure 2(b). Also increasing CFL number results in to a smoother approximation of the solution see Figure 2(c). It can also be observed from the results in Figure 2(a) and Figure 2(b) that induced oscillations at time $\tau = 0.01$ are not caused by the extrema at $x = 0$ in the initial condition but depends on the data ratio at the bottom corner (especially on left one at $x = -h$). We will see that such observation is well justified by Theorem 3.2 in section 3. Next we consider numerical results for impulsive initial

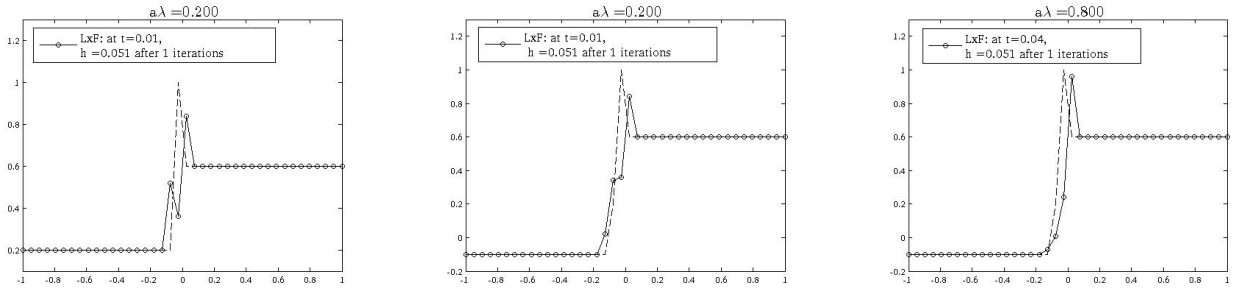

(a) (b) (c)

Figure 2: *Behavior of numerical oscillations by LxF scheme (5) for initial data sequence (shown by dashed line) with single extrema data (7) in (a), (8) in (b) and (c).*

condition (10) given in Figure 3 and Figure 4. It is clear from Figure 3 that for smaller CFL number, the solution is more oscillatory as reported in [9]. It can also be observed that for a fix h and fix number of iterations, changing $CFL = a\lambda$ affects the oscillatory behavior of LxF scheme see Figure 4, Figure 2(b) and 2(c). One possible explanation for higher magnitude of oscillations could be that for a fix CFL $\frac{a\tau}{h}$, larger space step h corresponds to larger time step τ. Thus scheme requires less iterations to reach desired time level and the obtained solution suffers from less artificial dissipation.

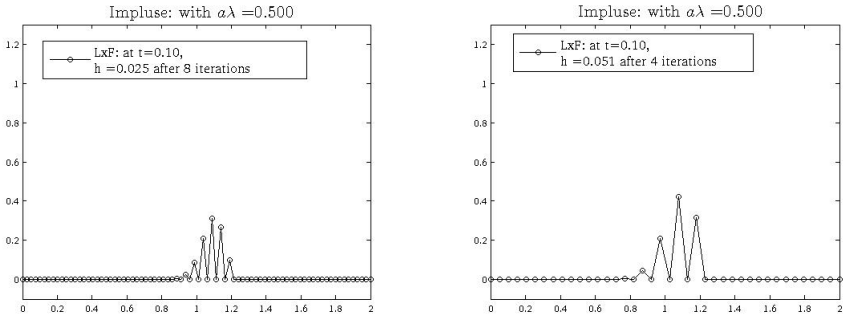

Figure 3: *Solution of transport equation (6) and initial condition (10). Amplitude of oscillations increase with larger step size h and fix $a\lambda$.*

Case (iii) *Step-wise approximation:* The discretization algorithm proposed in [2] preserves the number of extrema however *cause a step-wise approximation for discontinuous solution region* similar to Figure 5 (see also N-Wave solution of Burgers equation in [2]). Thus it is needed to have an algorithm which is independent of initial data discretization and can avoid such step wise approximation.

From above discussion based on existing literature, one can conclude that LxF scheme is *not always oscillatory for data extrema and depends locally on data type as well on CFL number or time step* τ contrary to claim in [3]. It motivates to analyse LxF scheme for stability in local sense.

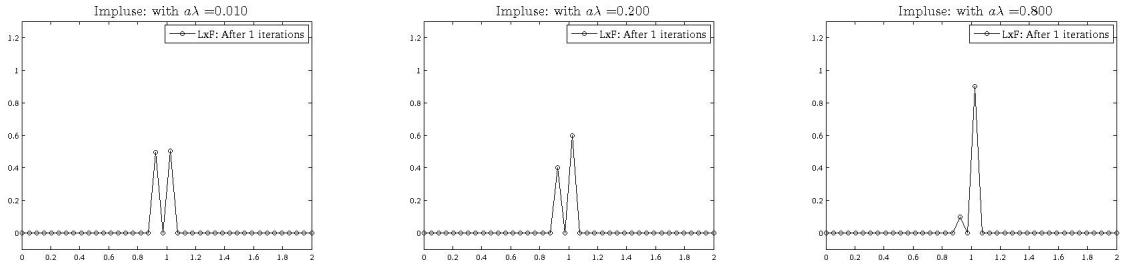

Figure 4: *Solution of transport equation (6) and impulsive initial condition (10). Effect of $a\lambda$ on oscillations even after one iteration*

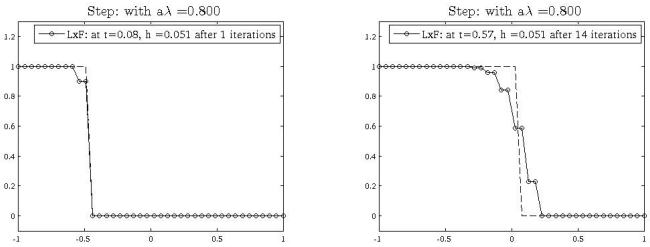

Figure 5: *Solution of transport equation (6) and initial condition (11). Step-wise approximation for discontinuous region*

3 Local maximum principle: a non-oscillatory condition

For clarity of the presentation consider the 1D transport equation (6) i.e.,

$$u_t(x,t) + a u_x(x,t) = 0,\ u(x,0) = u_0(x) \tag{12}$$

The method of characteristics suggest that solution $u(x,\tau)$ of conservation law (12) depends locally on solution value at previous time level i.e, $u(x,0)$[2]. Following it, in [7] a non-oscillatory stability condition known as local maximum principle is recently explored for (12). In discrete case is given by

$$\min_{x_{i-1}\le x\le x_i} u(x,t^n) \le u(x,t^{n+1}) \le \max_{x_{i-1}\le x\le x_i} u(x,t^n) \ \text{ if } \quad 0 \le a\lambda \le 1 \tag{13a}$$

$$\min_{x_i\le x\le x_{i+1}} u(x,t^n) \le u(x,t^{n+1}) \le \max_{x_i\le x\le x_{i+1}} u(x,t^n) \ \text{ if } -1 \le a\lambda \le 0 \tag{13b}$$

A numerical scheme for (12) which satisfies condition (13) ensures that the solution at time level t^{n+1} will be bounded by the solution at t^n with out introduction of a new local extremum and therefore also satisfies the global maximum principle (3). Note that, in interval of monotone solution $[x_a, x_b]$ we have [9],

$$\min_{x_a\le x\le x_b} u(x,t^n) = \min(u(x_a,t^n), u(x_b,t^n)) \tag{14a}$$

$$\max_{x_a\le x\le x_b} u(x,t^n) = \max(u(x_a,t^n), u(x_b,t^n)). \tag{14b}$$

[2]In fact $u(x,\tau) = u_0(x \pm \tau\, a) = u(x \pm \tau\, a, 0)$.

Thus for a two point scheme above non-oscillatory stable conditions (13) are satisfied if

$$\min(u_{i-1}^n, u_i^n) \le u_i^{n+1} \le \max(u_{i-1}^n, u_i^n) \text{ if } \quad 0 \le a\lambda \le 1 \tag{15a}$$

$$\min(u_i^n, u_{i+1}^n) \le u_i^{n+1} \le \max(u_i^n, u_{i+1}^n) \text{ if } -1 \le a\lambda \le 0 \tag{15b}$$

Using (15), construct a numerical discretization for (12) as

$$u_i^{n+1} = \begin{cases} \alpha u_i^n + \beta u_{i-1}^n & \text{if} \quad 0 \le a\lambda \le 1 \\ \alpha u_i^n + \beta u_{i+1}^n & \text{if} \quad -1 \le a\lambda \le 0 \end{cases} \tag{16}$$

where

$$\alpha \ge 0, \beta \ge 0, \ \alpha + \beta = 1 \text{ and } \beta = a\lambda. \tag{17}$$

Note that under condition (17), scheme (16) is a consistent approximation for (12). Moreover, a simple analysis shows that (16) is Von-Neumann stable under the condition $0 < \beta \le 1$. Therefore, according to Lax-Wendroff Theorem [11], the stable and consistent scheme (16) is convergent provided

$$\alpha \ge 0, \beta \ge 0, \ \alpha + \beta = 1 \text{ and } 0 < \beta \le 1. \tag{18}$$

Note that since $\alpha, \beta \ge 0$, $\alpha + \beta = 1$, the scheme (16) is essentially a convex combination of two grid values of $u(:, t^n)$ thus ensures that for a monotone data, the updated solution value of $u(:, t^{n+1})$ will remain bounded by both grid values without introducing of new local maxima-minima. This leads to the following definition

Definition 3.1. *Away from sonic point*[3]*, a numerical scheme written in form (16) is a consistent and non oscillatory stable approximation for (1) provided* $\alpha \ge 0, \beta \ge 0, \ \alpha + \beta = 1$ *and* $0 < \beta \le 1$.

In order to investigate the cause of induced local oscillations by LxF scheme (5), we analyze it for non-oscillatory stability condition (16). We assume that initial solution data at time level t^n does not contain a sonic point i.e., $a_{i+\frac{1}{2}}.a_{i-\frac{1}{2}} > 0$. In order to measure the smoothness of solution a function of consecutive gradients is used as in [19, 5, 6, 20]. It is given by

$$r_i = \begin{cases} \dfrac{\frac{u_i^n - u_{i-1}^n}{x_i - x_{i-1}}}{\frac{u_{i+1}^n - u_i^n}{x_{i+1} - x_i}} & \text{if} \quad a_{i+\frac{1}{2}} \ge 0 \\ \\ \dfrac{\frac{u_{i+1}^n - u_i^n}{x_{i+1} - x_i}}{\frac{u_i^n - u_{i-1}^n}{x_i - x_{i-1}}} & \text{if} \quad a_{i+\frac{1}{2}} \le 0 \end{cases} \tag{19}$$

In case of fixed mesh size, the Lax-Friedrich's scheme (5) can be written in the form

$$u_i^{n+1} = u_i^n - \frac{\lambda}{2}\left(f_{i+1}^n - f_i^n - \frac{1}{\lambda}(u_{i+1}^n - u_i^n) + f_i^n - f_{i-1}^n + \frac{1}{\lambda}(u_i^n - u_{i-1}^n)\right) \tag{20}$$

Let $a_{i+\frac{1}{2}}^n$ is the numerical approximation of characteristics speed $f^{'}(u)$, given by

$$a_{i\pm\frac{1}{2}} = \begin{cases} \dfrac{\Delta_\pm f(u_i^n)}{\Delta_\pm u_i^n} & \Delta_\pm u_i^n \ne 0 \\ \\ f^{'}(u_i^n) & else \end{cases} \tag{21}$$

[3]Sonic point is the one where characteristic speed changes its sign

where $\Delta_+ u_i^n = u_{i+1}^n - u_i^n = \Delta_- u_{i+1}^n$. Thus using (21), (20) reduced to

$$u_i^{n+1} = u_i^n - \frac{\lambda}{2}\left((a_{i+\frac{1}{2}}^n - \frac{1}{\lambda})(u_{i+1}^n - u_i^n) + (a_{i-\frac{1}{2}}^n + \frac{1}{\lambda})(u_i^n - u_{i-1}^n)\right) \tag{22}$$

Away from sonic point we have $f^{'}(u) \neq 0$ thus we have,
Case 1: Let $f^{'}(u) > 0$, (22) can be written in form (16) as

$$u_i^{n+1} = (1-\gamma)u_i^n + \gamma u_{i-1}^n,\ \gamma = \frac{1}{2}\left[(1+\lambda a_{i-\frac{1}{2}}^n) - (1-\lambda a_{i+\frac{1}{2}}^n)r_i^{-1}\right], \tag{23}$$

where $r_i^{-1} = \dfrac{(u_{i+1}^n - u_i^n)}{(u_i^n - u_{i-1}^n)}$. Under following conditions, scheme (23) is stable and non-oscillatory,

$$1 - \frac{1}{2}\left((1+\lambda a_{i-\frac{1}{2}}^n) - (1-\lambda a_{i+\frac{1}{2}}^n)r_i^{-1}\right) \geq 0,\ \forall i \tag{24a}$$

$$\frac{1}{2}\left((1+\lambda a_{i-\frac{1}{2}}^n) - (1-\lambda a_{i+\frac{1}{2}}^n)r_i^{-1}\right) \geq 0,\ \forall i \tag{24b}$$

which satisfies if

$$0 \leq \frac{1}{2}\left((1+\lambda a_{i-\frac{1}{2}}^n) - (1-\lambda a_{i+\frac{1}{2}}^n)r_i^{-1}\right) \leq 1$$

CFL condition $\lambda \max_u |f^{'}(u)| \leq 1$ implies $1 \pm \lambda a_{i+\frac{1}{2}} \geq 0,\ \forall i$. Thus the required condition on smoothness parameter to yield non-oscillatory stable approximation is

$$r_i^{-1} \geq -\frac{1-\lambda a_{i-\frac{1}{2}}}{1-\lambda a_{i+\frac{1}{2}}} \text{ and } r_i^{-1} \leq \frac{1+\lambda a_{i-\frac{1}{2}}}{1-\lambda a_{i+\frac{1}{2}}}$$

On inversion,

$$r_i \leq -\frac{1-\lambda a_{i+\frac{1}{2}}}{1-\lambda a_{i-\frac{1}{2}}} \text{ or } r_i \geq \frac{1-\lambda a_{i+\frac{1}{2}}}{1+\lambda a_{i-\frac{1}{2}}} \tag{25}$$

Case 2: Let $f^{'}(u) < 0$, we write (22) in form (15) as

$$u_i^{n+1} = (1+\gamma)u_i^n + \beta\gamma u_{i+1}^n,\ \gamma = \frac{1}{2}\left[(1-\lambda a_{i+\frac{1}{2}}) - (1+\lambda a_{i-\frac{1}{2}})r_i\right] \tag{26}$$

Similarly (26) is non-oscillatory provided

$$0 \leq \frac{1}{2}\left[(1-\lambda a_{i+\frac{1}{2}}) - (1+\lambda a_{i-\frac{1}{2}})r_i\right] \leq 1$$

On simplification

$$r_i \geq -\frac{1+\lambda a_{i+\frac{1}{2}}}{1+\lambda a_{i-\frac{1}{2}}} \text{ and } r_i \leq \frac{1-\lambda a_{i+\frac{1}{2}}}{1+\lambda a_{i-\frac{1}{2}}}$$

On inversion we get condition for LxF scheme (22) to be non-oscillatory stable as

$$r_i^{-1} \leq -\frac{1+\lambda a_{i-\frac{1}{2}}}{1+\lambda a_{i+\frac{1}{2}}} \text{ or } r_i^{-1} \geq \frac{1+\lambda a_{i-\frac{1}{2}}}{1-\lambda a_{i+\frac{1}{2}}} \tag{27}$$

Conditions (25) and (27) on smoothness parameter to yield non-oscillatory stable approximation show that LxF scheme is conditionally locally unstable. In other words,

Theorem 3.2. *LxF scheme (5) does not induces local oscillations and non-oscillatory stable for the solution region where measure of smoothness*

$$r_i \in \mathbb{S}^{LxF} = \begin{cases} \left(-\infty, -\dfrac{1-\lambda a_{i+\frac{1}{2}}}{1-\lambda a_{i-\frac{1}{2}}}\right] \cup \left[\dfrac{1-\lambda a_{i+\frac{1}{2}}}{1+\lambda a_{i+\frac{1}{2}}}, \infty\right) & if \quad 0 \leq \lambda a_{i+\frac{1}{2}} \leq 1 \\ \left(-\infty, -\dfrac{1+\lambda a_{i-\frac{1}{2}}}{1+\lambda a_{i+\frac{1}{2}}}\right] \cup \left[\dfrac{1+\lambda a_{i-\frac{1}{2}}}{1-\lambda a_{i+\frac{1}{2}}}, \infty\right) & if \quad -1 \leq \lambda a_{i+\frac{1}{2}} \leq 0 \end{cases} \tag{28}$$

where for the fixed mesh size (19) gives,

$$r_i = \begin{cases} \dfrac{u_i^n - u_{i-1}^n}{u_{i+1}^n - u_i^n} & if \quad a_{i+\frac{1}{2}} \geq 0 \\ \dfrac{u_{i+1}^n - u_i^n}{u_i^n - u_{i-1}^n} & if \quad a_{i+\frac{1}{2}} \leq 0 \end{cases} \tag{29}$$

Remark 1. The non-oscillatory conditions in (28) can be alternatively derived by putting LxF in incremental form

$$u_i^{n+1} = u_i^n - C_{i-\frac{1}{2}}(u_i^n - u_{i-1}^n) + D_{i-\frac{1}{2}}(u_{i+1}^n - u_i^n) \tag{30}$$

which is TVD if $C_{i-\frac{1}{2}} \geq 0,\ D_{i+\frac{1}{2}} \geq 0$ and $C_{i+\frac{1}{2}} + D_{i+\frac{1}{2}} \leq 1,\ \forall i$. For example, in case of $f^{'}(u) \geq 0$, by choosing the coefficients of incremental LxF as

$$C_{i-\frac{1}{2}} = \frac{1}{2}\left((1+\lambda a_{i-\frac{1}{2}}^n) - (1-\lambda a_{i+\frac{1}{2}}^n)\frac{(u_{i+1}^n - u_i^n)}{(u_i^n - u_{i-1}^n)}\right), D_{i+\frac{1}{2}} = 0$$

.

Remark 2. From Theorem 3.2 and Remark 1, it can be concluded that LxF is locally unstable and therefore introduce local oscillations.

3.1 Further discussion

In order to explain the issues raised in Subsection 2.1, we consider the following corollary for the transport equation (6).

Corollary 3.3. *Under CFL condition* $0 \leq a\lambda \leq 1$ *LxF is locally oscillatory and unstable if the smoothness parameter* $r_i \in \left(-1, \dfrac{1-a\lambda}{1+a\lambda}\right)$.

Geometrically the region of instability for LxF scheme is shown in Figure 6. It shows the direct dependence of induced oscillations on CFL number. Larger CFL number $a\lambda$ reduces the region of instability from $(-1, 1)$ to $(-1, 0)$ which explain the nature of induced oscillations in Figure 4 in Subsection 2.1. Note that the presence of a extrema in solution corresponds to negative measure of smoothness i.e., $r < 0$. Corollary 3.3 shows that LxF does not introduce oscillations for those points of extrema where $r \leq -1$. It also justify the non-occurrence of induced oscillations at smooth extrema where $r \approx -1$ as in case (i), Figure 1 of Subsection 2.1. Further, we observed that numerical oscillations induced by LxF scheme are significantly visible in the solution region where smoothness parameter is close to zero i.e., $r \to 0$. It is elaborated through numerical examples in subsection 4.4.

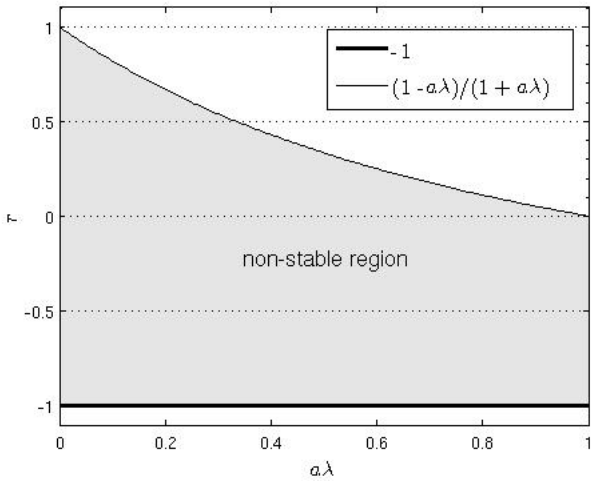

Figure 6: *Larger CFL number $a\lambda$ corresponds to smaller instability interval for LxF scheme*

4 Computational results

In order to validate the stability region $\mathbb{S}^{LxF}$ for LxF scheme as given in Theorem 3.2, it is sufficient to consider scalar test problems similar to the ones taken in [2, 14][4]. Computational results are presented by LxF scheme and a hybrid approach defined as: if $r_i \notin \mathbb{S}^{LxF}$ use first order upwind scheme otherwise use LxF scheme i.e.,

$$u_i^{n+1} = u_i^n - \chi(r_i^n)\Delta_- F_{i+\frac{1}{2}}^{LxF} - (1 - \chi(r_i^n))\,\Delta_- F_{i+\frac{1}{2}}^{UP} \tag{31}$$

where $F_{i+\frac{1}{2}}^{LxF}$ and $F_{i+\frac{1}{2}}^{UP}$ denotes the numerical flux function of LxF and first order upwind scheme respectively. The switch function χ is defined as

$$\chi(r_i^n) = \begin{cases} 1 & \text{if } r_i^n \in \mathbb{S}^{LxF}, \\ 0 & \text{else.} \end{cases} \tag{32}$$

Computed results obtained by this approach are labelled as $UpLxF$ whereas solution by LxF alone is labelled as LxF. In order to avoid computational overflow smoothness parameter r_i is computed in case of positive wave speed as

$$r_i = \begin{cases} 1 & \text{if } (\Delta_- u_i^n)^2 + (\Delta_+ u_i^n)^2 < \epsilon, \\ \dfrac{\Delta_- u_i^n}{\Delta_+ u_i^n} & \text{if } \Delta_+ u_i^n > \epsilon, \\ \left(\dfrac{\Delta_- u_i^n}{\epsilon}\right) sign(\Delta_+ u_i^n) & \text{else,} \end{cases}$$

where $\epsilon > 0$ is small tolerance. Analogously r_i is calculated for negative wave speed.

4.1 1D linear transport

Consider the transport equation (6) and the impulse and step wise initial conditions (10) and (11) respectively. For impulsive initial condition, in Figure 7, numerical results are given for fix CFL

[4]Similar results are observed in case of systems.

number $a\lambda$ with varying space step h. In Figure 8 results are given for fix number of iterations and fix space step h and varying $a\lambda$.

Results in Figure 7 and Figure 8 show that LxF does not introduces oscillations when applied in solution region corresponding to its stability interval. In Figure 9 numerical results are given for step wise initial condition (11). It can be seen that oscillations or step-wise approximation is completely removed even after one iteration by $UpLxF$ approach.

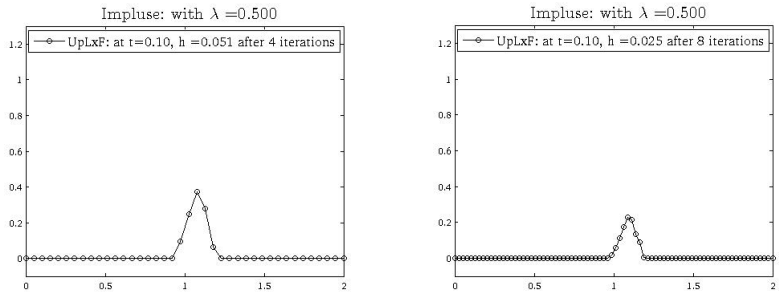

Figure 7: *Linear transport problem: Impulsive initial condition (10). No oscillations though increased amplitude with larger step size h and fix $a\lambda$ due to less iterations.*

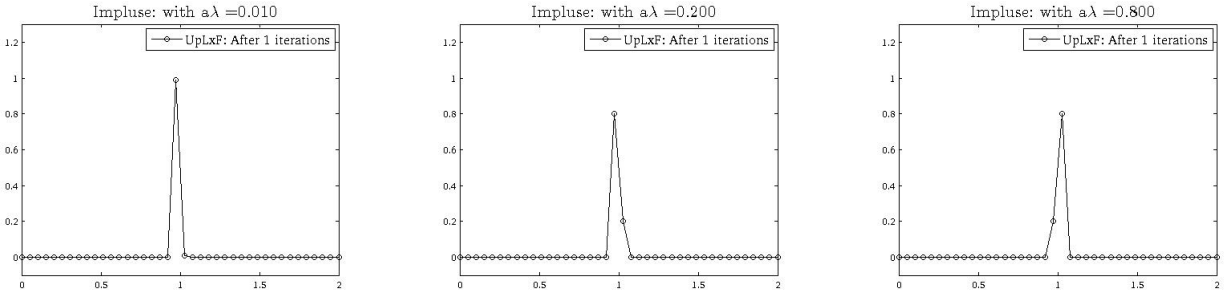

Figure 8: *Linear transport problem: Effect of $a\lambda$: Fix iteration but no induced oscillation by hybrid approach*

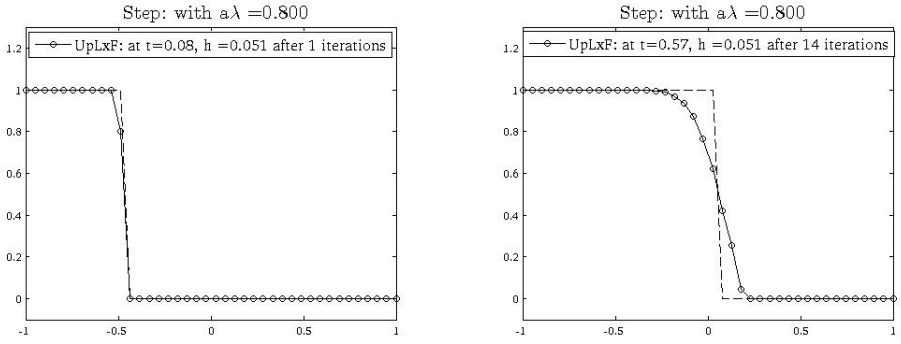

Figure 9: *Solution of transport equation (6) with initial condition (11). monotone approximation for discontinuous region with hybrid approach*

4.2 2D linear transport

We consider 2D scalar problem

$$u(x,y,t)_t + u(x,y,t)_x + u(x,y,t)_y = 0,\ (x,y) \in [0,1] \times [0,1] \tag{33}$$

along with the initial condition

$$u(x,y) = \begin{cases} \sin^2(\pi\, x)\sin^2(\pi\, y) & \text{if } y \le x, \\ 0 & \text{else,} \end{cases} \tag{34}$$

The exact solution for this problem move along with $y = x$ line with out loosing its initial shape. Results in Figure 10 shows that LxF induces local oscillations around extrema where as UpLxF approach completely removes such induced oscillations.

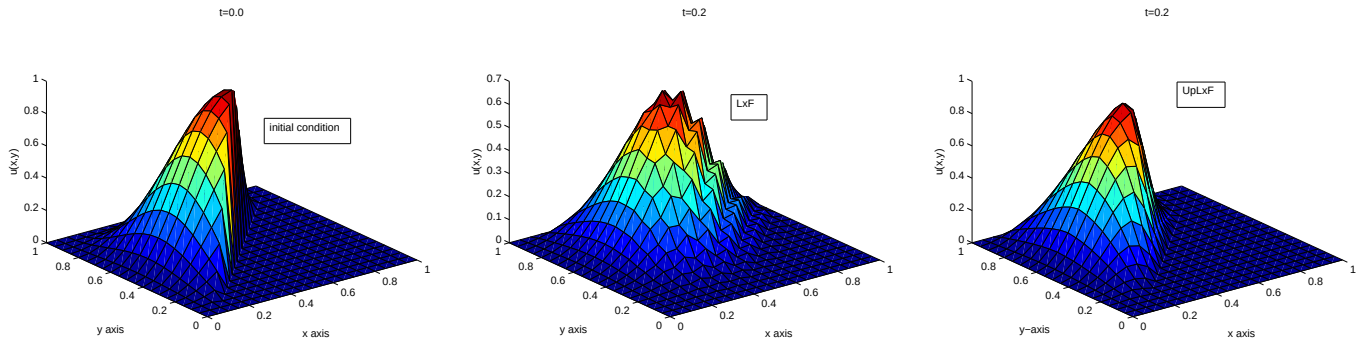

(a) (b) (c)

Figure 10: 2 dimensional transport: (a) initial condition, (b) solution by LxF scheme, (c) solution by UpLxF approach.

4.3 Non-linear Burgers equation

In order to show that occurrence of induced oscillations by LxF scheme for non-linear case we take the Burgers equation

$$u_t + \left(\frac{u^2}{2}\right)_x = 0, \tag{35}$$

along with the initial conditions from [2],

$$u_0(x) = \begin{cases} \frac{x-10}{2} & 10 \le x \le 12, \\ 0 & else. \end{cases},\ x \in [5,15]. \tag{36}$$

The exact solution at time t is N-wave and given by

$$u_N(x,t) = \begin{cases} \frac{x-10}{t+2} & 10 \le x \le 10 + \sqrt{2(t+2)} \\ 0 & else \end{cases} \tag{37}$$

In this case LxF shows oscillatory approximation for N-wave solution Figure 11 (left). The numerical approximation by UpLxF approach completely removes such oscillations see Figure 11. Also the $UpLxF$ approach does not show step-wise approximation for N-wave.

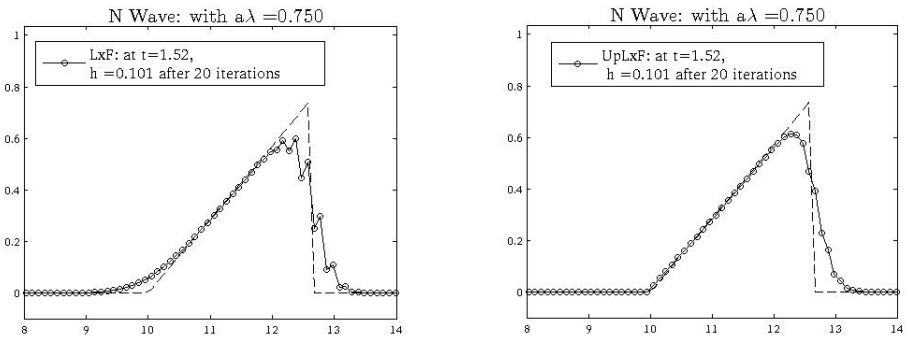

Figure 11: *N-wave solution of Burgers equation corresponding to initial condition (36). Induced local oscillations by LxF scheme (left) while no induced oscillation with hybrid approach (right)*

4.4 Oscillations corresponds to $r \approx 0$

We show that induced oscillations are mainly caused by solution data region where smoothness parameter (29) falls in the vicinity of zero. Note that $r \to 0^-$ indicates extrema whereas $r \to 0^+$ indicates steep monotone gradient region. In order to validate it we apply first order Upwind scheme only at those grid point x_i where $|r_i| < \delta$ otherwise LxF scheme is applied. To be precise we used UpLxF with switch function

$$\chi(r_i^n) = \begin{cases} 1 & \text{if } |r_i^n| > \delta, \\ 0 & \text{else.} \end{cases} \tag{38}$$

For the computations tolerance δ is chosen as $\delta = 1e^{-8}$. We reconsider the linear transport equation (6) and Burgers equation (35) along with step wise initial condition (11) and N-wave initial condition (36) respectively. The numerical result obtained by this approach is denoted by *iter*. Numerical results are given in Figure 12 and Figure 13 which show that oscillations and step-wise approximation are completely removed when first upwind scheme is applied only in the region where $|r| < \epsilon$. This shows that oscillations are not only caused at extrema but also at steep gradient region of solution. We characterize that *oscillations by LxF scheme are caused only at those data extrema where* $-1 << r < 0$ *and at steep gradient region of solution where* $0 < r << 1$ *e.g., strictly increasing/decreasing high gradient monotone data.*

5 Conclusion

A simple proof in terms of bounds on smoothness parameter is given to show that LxF scheme is locally unstable. Characterization are done e.g., type of data extrema and solution region which cause such induced oscillations, effect of CFL number on induced oscillations by LxF scheme. Detailed numerical results are shown and discussed to support the claims.

References

[1] Jay P Boris and David L Book. Flux-corrected transport. i. shasta, a fluid transport algorithm that works. *Journal of Computational Physics*, 11:38–69, 1973.

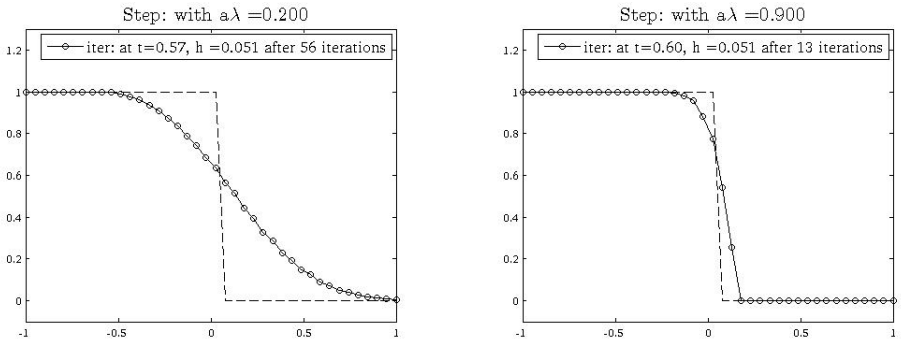

Figure 12: *Linear transport equation with step wise initial condition (11): No induced local oscillations by LxF when applied in solution region* $|r_i| > \epsilon$.

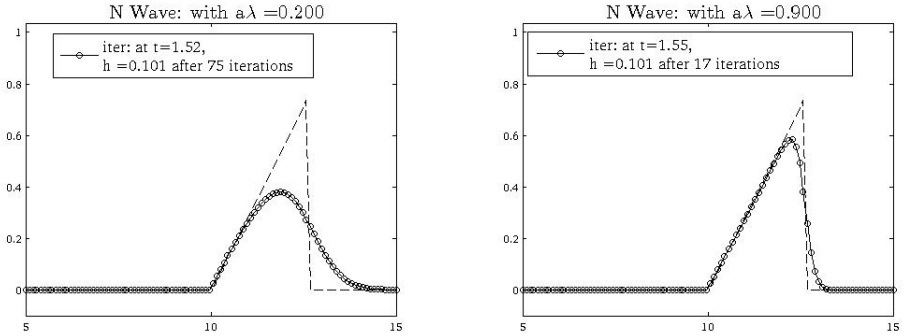

Figure 13: *N-wave solution of Burgers equation corresponding to initial condition (36). LxF does not show induced oscillation when applied in region* $|r_i| > \epsilon$.

[2] M. Breuß. The correct use of the lax-friedrichs method. *ESAIM: Mathematical Modelling and Numerical Analysis, M2AN*, pages 519–540, 2004.

[3] M. Breuß. An analysis of the influence of data extrema on some first and second order central approximations of hyperbolic conservation laws. *ESAIM: Mathematical Modelling and Numerical Analysis*, 39(5):965–994, 2005.

[4] M G Crandall and A Majda. Monotone difference approximations for scalar conservation laws. *Mathematics of Computation*, 34:1–21, 1980.

[5] Ritesh Kumar Dubey. Flux limited schemes: Their classification and accuracy based on total variation stability regions. *Applied Mathematics and Computation*, 224:325–336, 2013.

[6] Ritesh Kumar Dubey. Total variation stability and second-order accuracy at extrema. *Electron. J. Diff. Eqns.*, 20:53–63, 2013.

[7] Ritesh Kumar Dubey, Biswarup Biswas, Vikas Gupta, Local maximum principle satisfying high order non-oscillatory schemes, accepted for publication in International Journal for Numerical Methods in Fluids, DOI:10.1002/fld.4202.

[8] C B Laney and David Caughey. *Extremum control. II - Semidiscrete approximations to conservation laws*. Aerospace Sciences Meetings. American Institute of Aeronautics and Astronautics, Jan 1991.

[9] Culbert B. Laney. *Computational gasdynamics*. Cambridge University Press, 1998.

[10] Peter D. Lax. Weak solutions of non-linear hyperbolic equations and their numerical approximation. *Communications in Pure and Applied Mathematics*, 7:159–193, 1954.

[11] Peter D Lax and B Wendroff. Systems of conservation laws. *Comm. Pure. Appl. Math.*, 13:217–237, 1960.

[12] Philip G Lefloach and J G Liu. Generalized monotone schemes, discrete paths of extrema and discrete entropy conditions. *Mathematics of Computation*, 68:1025–1055, 1999.

[13] Randall J. LeVeque. *Numerical Methods for Conservation Laws*. Lectures in mathematics ETH Zürich. Birkhäuser Basel, 2nd edition, February 1992.

[14] Jiequan Li, Huazhong Tang, Gerald Warnecke, and Lumei Zhang. Local oscillations in finite difference solutions of hyperbolic conservation laws. *Mathematics of Computation*, 78:pp 1997–2018, 2009.

[15] Jiequan Li and Z Yang. Heuristic modified equation analysis of oscillations in numerical solutions of conservation laws. *SIAM J. Num. Analysis*, 49:2386–2406, 2011.

[16] H. Nessyahu and E. Tadmor. Non-oscillatory central differencing for hyperbolic conservation laws. *Journal of Computational Physics*, 87:408–436, 1990.

[17] Stanly Osher and Etan Tadmor. On the convergence of difference approximations to scalar conservation laws. *Mathematics of Computation*, 50:19–51, 1988.

[18] R Sanders. On the convergence of monotone finite difference schemes with variable spatial differencing. *Mathematics of Computation*, 40:91–106, 1983.

[19] P. K. Sweby. High resolution schemes using flux limiters for hyperbolic conservation laws. *Siam Journal on Numerical Analysis*, 21(5):995–1011, 1984.

[20] E. F. Toro. *Riemann Solvers and Numerical Methods for Fluid Dynamics: A Practical Introduction*. Springer, 3rd edition, April 2009.

[21] Xiangxiong Zhang and Chi-Wang Shu. On maximum-principle-satisfying high order schemes for scalar conservation laws. *Journal of Computational Physics*, 229(9):3091 – 3120, 2010.